

Acoustic thermometry for detecting quenches in superconducting coils and conductor stacks

M. Marchevsky and S. A. Gourlay

Citation: *Appl. Phys. Lett.* **110**, 012601 (2017); doi: 10.1063/1.4973466

View online: <http://dx.doi.org/10.1063/1.4973466>

View Table of Contents: <http://aip.scitation.org/toc/apl/110/1>

Published by the [American Institute of Physics](#)

Articles you may be interested in

[Stripe magnetic domains in CeY₂Fe₅O₁₂ \(Ce:YIG\) epitaxial films](#)

Appl. Phys. Lett. **110**, 012406 (2017); 10.1063/1.4973481

[Realization of compact tractor beams using acoustic delay-lines](#)

Appl. Phys. Lett. **110**, 014102 (2017); 10.1063/1.4972407

[Sub 250 nm deep-UV AlGaIn/AlN distributed Bragg reflectors](#)

Appl. Phys. Lett. **110**, 011105 (2017); 10.1063/1.4973581

[Mathematical operations for acoustic signals based on layered labyrinthine metasurfaces](#)

Appl. Phys. Lett. **110**, 011904 (2017); 10.1063/1.4973705

Acoustic thermometry for detecting quenches in superconducting coils and conductor stacks

M. Marchevsky and S. A. Gourlay

Lawrence Berkeley National Laboratory, Berkeley, California 94720, USA

(Received 27 September 2016; accepted 16 December 2016; published online 5 January 2017)

Quench detection capability is essential for reliable operation and protection of superconducting magnets, coils, cables, and machinery. We propose a quench detection technique based on sensing local temperature variations in the bulk of a superconducting winding by monitoring its transient acoustic response. Our approach is primarily aimed at coils and devices built with high-temperature superconductor materials where quench detection using standard voltage-based techniques may be inefficient due to the slow velocity of quench propagation. The acoustic sensing technique is non-invasive, fast, and capable of detecting temperature variations of less than 1 K in the interior of the superconductor cable stack in a 77 K cryogenic environment. We show results of finite element modeling and experiments conducted on a model superconductor stack demonstrating viability of the technique for practical quench detection, discuss sensitivity limits of the technique, and its various applications. *Published by AIP Publishing.* [<http://dx.doi.org/10.1063/1.4973466>]

A robust and reliable detection of spontaneous quenching is essential for protecting superconducting magnets and machinery from thermal damage. For coils made of high-temperature superconductors (HTS), sensitivity of the conventional quench detection approach based on measuring resistive voltages may be insufficient to detect hot spots early enough, especially in large systems exhibiting a high level of electromagnetic noise. This is because quench propagation velocity in HTS conductors is 2–3 orders of magnitude lower than in conventional superconductors,^{1,2} and a normal zone may heat up significantly before any resistive voltage across it becomes measurable. Here, we propose and demonstrate an alternative method for detecting quenches in HTS conductor stacks (such as coil windings, cables, etc.) based on monitoring their internal temperature with acoustic waves. Our approach is non-invasive, as it relies upon instrumentation placed outside of the stack interior. It is largely insensitive to electromagnetic and mechanical noise in the system—in contrast to the passive acoustic quench detection techniques^{3–5} aimed at analyzing sound emission from the quench zone. Our method also differs from the earlier proposed quench detection strategies^{6–8} relying upon measuring local thermally induced stresses, and thus allows to decouple stress and thermal monitoring for the same object.

Acoustic thermometry is presently well-established in application to liquids and gaseous bodies.^{9,10} It relies upon measuring a thermally induced change of the sound velocity $c(T)$. Such measurement can be accomplished by generating an acoustic pulse, and measuring its travel time across the body. Piezoelectric transducers can be used for transmitting and receiving such pulses, having either two transducers—a transmitter and a receiver placed at the opposite sides of the body, or a single transducer in a pulse-echo operating mode.¹¹ However, this simple approach is not very practical for application to solids. For example, in a quasi-one-dimensional solid rod, the transverse sound velocity is $v = \sqrt{\frac{E}{\rho}}$, and its temperature dependence is dominated by that of the

Young's modulus $E(T)$ rather than a much smaller density variation $\rho(T)$. The former can be approximated as¹²

$$E(T) = E_0 - s/[e^{\frac{t}{T}} - 1], \quad (1)$$

where E_0 is the zero-temperature value, and s and t are adjustable parameters. For common metals and alloys at liquid nitrogen temperature (77 K), the relative change $1 - E(T + \Delta T)/E(T)$ is then just $\sim 1 \times 10^{-4} \text{ K}^{-1}$, yielding a ~ 2 – 3 orders of magnitude smaller sound velocity change per degree than in liquids or gases. Another significant complication is that a large variety of wave modes exist in solids, including compression, shear, twist, and Lamb surface waves. Those wave modes exhibit different group velocities¹³ and can evolve from one mode to another along the body surfaces and interfaces. Once a solid body is excited with a pulsed mechanical excitation at t_0 , it would “ring down,” yielding multiple transient oscillations and wave mode conversions before the initial pulse energy is fully dissipated into heat. A superposition of eigenmodes corresponding to the body's structural degrees of freedom will dominate its transient response once waves have bounced repeatedly from external boundaries and internal interfaces. The resulting spatio-temporal distribution of the deformation is then uniquely defined by the density and Young's modulus distribution in the body while the time decay of the transient response is proportional to the rate of mechanical energy loss. Transients can be excited and monitored for changes repeatedly, provided that the interval between the excitation pulses is longer than the transient decay time. Should a sudden structural change, such as cracking or delamination inside an epoxy-impregnated coil occur, for example, the transient waveform shape will change drastically.¹⁴ This phenomenon constitutes the basis for various non-destructive evaluation techniques.^{11,15} A much more subtle yet continuous thermally induced variation of the transient is expected due to a temperature dependence of elastic constants, since eigenfrequencies follow the same square-root functional

dependence upon Young's modulus¹⁶ as does the sound velocity. One can therefore expect a similar 10^{-4} – 10^{-5} K⁻¹ magnitude of thermal frequency shift of the mechanical modes comprising the transient. To detect a shift this small, one can rely upon the body's fairly large mechanical Q-factor (defined as a number of transient oscillation periods over which their amplitude decreases by a factor of $e^{-\pi}$), typically ranging from $\sim 10^2$ at ambient conditions to $\sim 10^3$ at cryogenic temperatures for most metallic structures. For single-mode resonators, such as electromechanical quartz resonators, for example ($Q \sim 10^4$ at room temperature and $> 10^6$ at 4.2 K), thermal frequency shifts can be monitored in either a continuous oscillation¹⁷ or a pulsed transient mode.¹⁸ But for a structurally complex object such as a superconducting magnet coil where a large variety of mechanical modes can be excited simultaneously, monitoring changes in its overall transient response is a more practical approach. To quantify such changes, we apply an excitation pulse to the body at t_0 and acquire a fixed portion of the transient waveform of a duration t_w starting at $t_0 + \Delta t$. The first acquired waveform $f_0(t)$ is stored as a reference and then cross-correlated with every subsequently-acquired waveform $f_i(t)$ to find

$$F_i(t) = \int_{t_0 + \Delta t}^{t_0 + \Delta t + t_w} f_i(t - x) f_0(t) dx. \quad (2)$$

The relative time shift τ_i is then calculated, corresponding to the absolute maximum of each $F_i(t)$ in the $[-0.5t_w, 0.5t_w]$ interval, such as that $F_i'(\tau_i) = 0$; $F_i''(\tau_i) < 0$. Thermal sensitivity is expected to be proportional to Δt , and thus, one can benefit from the large mechanical Q-factor by increasing Δt further into the "tail" of the transient waveform. A similar waveform monitoring approach was proposed¹⁹ for thermal mapping of biological tissues with medical ultrasound.

We have conducted a finite-element transient simulation in ANSYS for a model system that resembles a section of a flat coil wound with a tape conductor. It consists of eleven $100 \mu\text{m}$ -thick stainless tapes inter-separated by ten $25 \mu\text{m}$ -thick polyethylene tapes stacked together. The tape stack is sandwiched between two 1-mm thick copper plates. The assembly length is 120 mm, and its width is 12 mm. Solid (aka "frozen") contacts between all constituent parts are considered. Two round piezoelectric transducers are placed at the outer surfaces of the top and bottom copper plates, respectively. The transducers are modelled as 0.1 mm-thick disks, 6 mm in diameter placed along the middle line of the tapes at a 25 mm distance from the ends of the stack. They are assumed to have an isotropic Young's modulus of 9.6×10^{10} Pa, Poisson ratio of 0.36, polarization constant $d_{33} = 15.1 \text{ C/m}^2$, and the polarization direction aligned with the transverse axis of the stack. The transmitting transducer is energized with a $0.2 \mu\text{s}$ -long rectangular 10 V pulse and the transient displacement as well as the voltage across the receiving transducer is calculated for the interval of $600 \mu\text{s}$ using a constant time step of $0.2 \mu\text{s}$. Two simulations were performed: one for an unmodified stack using reference material parameters (at a base temperature of 295 K), and another one for a modified stack where the Young's modulus E of the middle (6th) stainless tape was decreased along

its entire length by 1% relative to the initial value of 1.93×10^{11} Pa in order to emulate the effect of a temperature rise. The results of transient displacement calculation are shown in Fig. 1. As the initial excitation propagates away from the transmitter, various volumetric and lateral eigenmodes are excited, eventually leading to a formation of a complex time-varying displacement pattern across the stack volume. The voltage across the receiver transducer for the unmodified stack is plotted in Fig. 2(a). The transducer was assumed to be grounded at the side bonded to the copper plate, and the plotted voltage is the average $(V_{\min} + V_{\max})/2$ taken across its outer surface at each step of the calculation. The transient exhibits a prevailing frequency centered at ~ 860 kHz, and a complex envelope pattern resulting from interference of multiple wave modes. Same transient waveform was calculated for the modified stack, and then two sub-waveforms were selected from each transient. They were compared directly and also using the cross-correlation method (2). For the two sub-waveforms selected at $t = 45 \mu\text{s}$, their relative time shift appears to be negligible. However, for the two selected further into the transient (at $t = 595 \mu\text{s}$), a measurable relative time shift is seen, corresponding to an increase in the oscillation period τ for the modified stack. In Fig. 2(c), the relative time shift $\tau(t)$ calculated using (2) for the corresponding sub-waveform blocks of $t_w = 20 \mu\text{s}$ of the

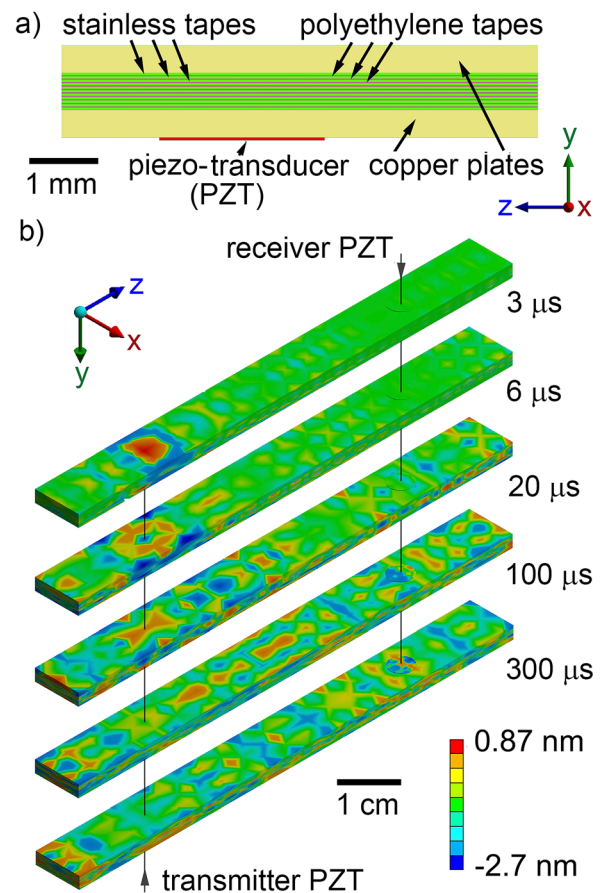


FIG. 1. (a) A portion of the tape stack assembly (in cross-section) chosen for ANSYS modeling. (b) Results of ANSYS simulation of the transient displacement in the stacked tape assembly in response to a pulsed mechanical excitation applied at $t = 0.2 \mu\text{s}$, shown for the five different simulation times denoted in the image. The color map represents distribution of directional deformation along the normal ("y") axis of the stack assembly.

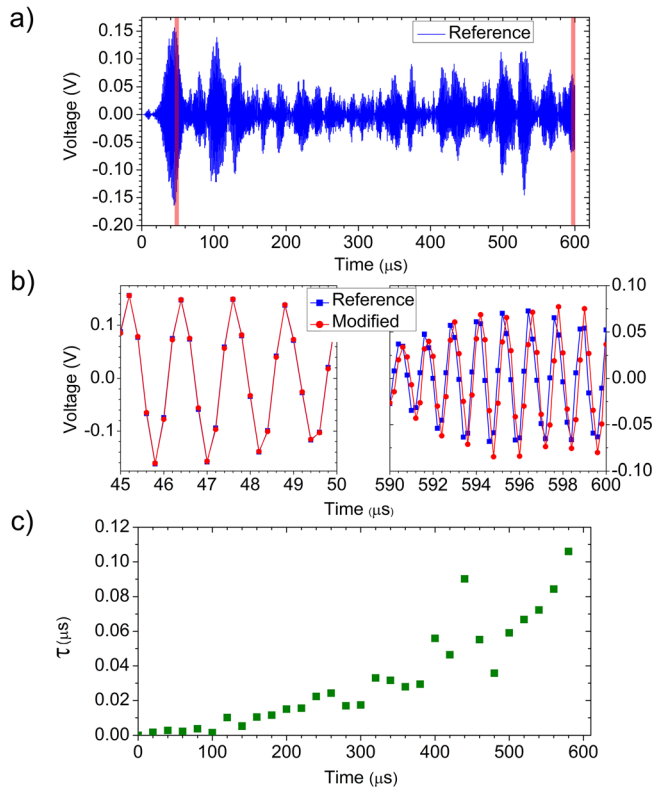


FIG. 2. (a) Voltage waveform at the receiving transducer calculated for the reference (unmodified) stack assembly. Two sub-waveforms of duration $t_w = 5 \mu\text{s}$ were selected (marked in the graph) for comparison to those of the modified stack. (b) Left: the sub-waveforms starting at $45 \mu\text{s}$ into the transient (show their good mutual registry). Right: the sub-waveforms starting at $595 \mu\text{s}$ into the transient (show an accumulated systematic time shift). (c) Time shift $\tau(\tau)$ between the transient sub-waveforms of the reference and modified stack assembly.

reference and modified transient is plotted. The origin of the observed roughly quadratic character of $\tau(t)$ requires further investigation by varying structural parameters of the system, and possibly modifying the simulation time step. The assumed $\Delta E/E = 0.01$ for stainless steel corresponds to a temperature rise of $\sim 25 \text{ K}$, which would constitute a rather large thermal detection threshold for a real HTS conductor stack. This variation magnitude was simply chosen to reduce the simulation time. However, as the result of Fig. 2(c) shows, $\tau(\tau)$ accumulated over $\sim 600 \mu\text{s}$ of the transient corresponds to a substantial phase shift of 31° at 860 kHz , suggesting a potentially large temperature sensitivity margin. It should be noted that the transient time shift is expected to be additive over any thermally perturbed volume;²⁰ we therefore expect this simulation to provide a correct order of magnitude estimate also in case of a localized “hot spot.”

To validate our technique as a quench detection tool, we tested it experimentally using a stacked tape assembly built around a practical HTS tape conductor. The conductor (type SCS12050, from SuperPower, Inc.) had $\sim 1 \mu\text{m}$ -thick yttrium barium copper oxide (YBCO) layer deposited on buffer layers on top of the 12-mm wide Hastelloy substrate, and stabilized by a surrounded silver and copper stabilizer of $40 \mu\text{m}$ overall thickness. The net thickness of the HTS tape was $\sim 100 \mu\text{m}$. To define the artificial “hot spot,” two notches were made in the stabilizer and YBCO layers, thus forming a locally reduced path for the current (Fig. 3(a)). The conductor was then stacked

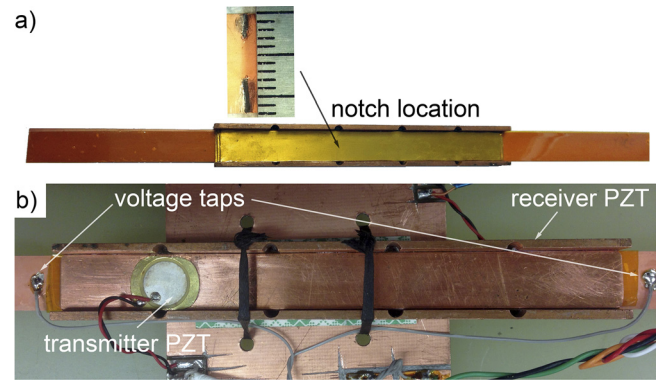


FIG. 3. (a) Top view of the stack at an intermediate stage of the assembly process. An artificial defect (two notches, as shown in the inset) was made in the tape to locally reduce path for the current. (b) A photograph of the completed stack assembly mounted at the cryostat inset for testing at 77 K .

with five 12 mm-wide and $100 \mu\text{m}$ -thick stainless tapes at each side, having an adhesive $25 \mu\text{m}$ -thick Kapton foil placed in-between the adjacent tapes. The entire stack was bonded layer-by-layer using cyanoacrylate glue, placed and bonded inside a rectangular shaped copper channel, and a 1 mm-thick copper plate was added at the top. Two piezo-transducers made of $100 \mu\text{m}$ -thick transversely polarized lead-strontium-titanate film deposited on $150 \mu\text{m}$ -thick bronze disks of 1 cm in diameter were glued at the opposite sides of the assembly, at 5 cm from its ends. The HTS conductor was spliced to the current leads using six 0.1 mm-thick copper tapes at each end, three tapes at each conductor side. Voltage taps were soldered at the YBCO side $\sim 1 \text{ cm}$ from the conductor ends. The completed assembly is shown in Fig. 3(b).

The tests were conducted in a liquid nitrogen bath. Rectangular voltage pulses of 14 V amplitude were applied to the transmitter transducer at a rate of 9 Hz using a HP8116A function generator. The excitation pulse duration was set to $7.2 \mu\text{s}$, which yielded the largest amplitude and longest observed ringing down of the transient waveform. The latter was recorded directly from the receiver transducer by an OWON SDS7201V oscilloscope at a 40 MHz sampling rate (Fig. 4(a)). The prevailing frequency component of the transient was $\sim 200 \text{ kHz}$. Next, a reference sub-waveform of $75 \mu\text{s}$ duration was selected starting at $\sim 220 \mu\text{s}$ from the leading edge of the excitation pulse. It was re-acquired and averaged 10 times; the resulting waveform was stored and then continuously monitored for time shift $\tau(\tau)$ using the algorithm (2) implemented with LabView software. Initially, $\tau(t)$ was monitored for $\sim 100 \text{ s}$ at zero driving current, and it did not show a notable change fluctuating in the $\pm 0.03 \mu\text{s}$ range. Boiling nitrogen in the cryostat did not seem to affect the signal. Next, current was applied to the tape conductor in a linear ramp fashion at a rate of 1.37 A/s , and the voltage between the taps was measured using a Keithley 2182A Nanovoltmeter. Results of the simultaneous τ and voltage measurement as function of time are shown in Fig. 4(b), while the same results as function of the driving current are shown in Fig. 4(c). As the current increases, the resistive voltage across the conductor becomes detectable at $\sim 120 \text{ A}$ and reaches $1 \mu\text{V}$ at 143 A . At the same time, $\tau(\tau)$ starts to increase monotonically with current at around 80 A , reaching

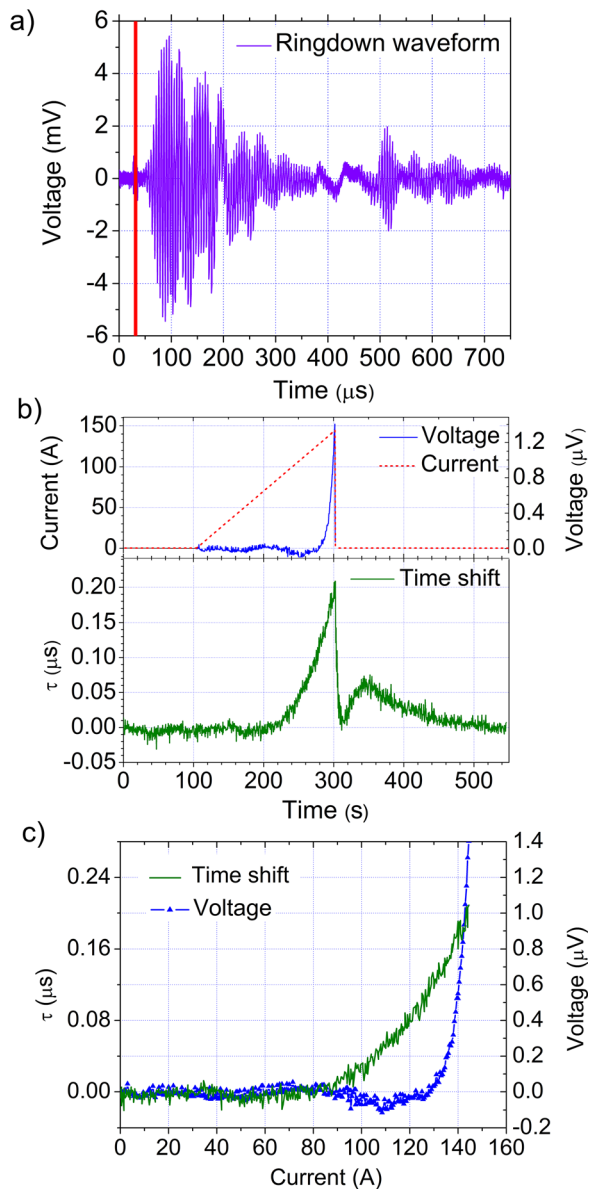


FIG. 4. (a) A transient waveform acquired by the receiving transducer. The time window of the excitation pulse is shown in the graph with the red line. A prevailing ringdown frequency component of the transient is centered at ~ 200 kHz. (b) Top: voltage across the HTS conductor measured during a linear current ramp. Bottom: Time shift τ for the transient sub-waveform acquired during the same current ramp. (c) Time shift τ and voltage across the conductor plotted versus the applied current.

$\sim 0.2 \mu\text{s}$ peak value at the maximum current of 143 A. Once the current is switched off, $\tau(\tau)$ jumps down quickly, partly recovers, and then follows a transitional decay for ~ 140 s towards its initial level prior to the current ramp. The slow decay may be related to a cooling of the stack interior, and spatial re-distribution of the deposited heat. The entire experiment was then repeated, yielding the same magnitude of the time shift, and a fully reproducible current-voltage characteristic of the conductor. When compared to the prevalent period of the transient, the measured peak of $\tau(t)$ during the resistive transition in the HTS conductor corresponds to 14° of net phase shift with respect to the reference sub-waveform. Given that ~ 45 transient oscillation have taken place in the $220 \mu\text{s}$ prior to the accumulated sub-waveform, this translates into $\sim 8 \times 10^{-4}$ of the relative frequency shift

for the most prominent (200 kHz) vibrational eigenmode of the stack assembly. Notably, the $\tau(t)$ rise precedes the voltage rise, and in fact coincides with an onset of a small $-0.1 \mu\text{V}$ voltage across the tape appearing at ~ 90 A. Such a “reversed” voltage anomaly in a current-voltage characteristic of HTS tape is often associated with the resistive transition that occurs outside of the segment between the voltage taps, but diverts some current into the stabilizer layer of that segment due to a finite current diffusion length.²¹ The net heat release in the conductor estimated as power integrated over the duration of the ramp is ~ 1.27 mJ. By using temperature-dependent values for the heat capacities of the conductor materials, and assuming the normal zone length along the tape of 1 mm, this heat amount yields a local temperature rise of ~ 0.6 K (or a proportionally smaller number for a larger-sized normal zone) in adiabatic approximation. Based on (1) and the reference Young’s modulus values for the conductor materials, the relative eigenfrequency change corresponding to such temperature variation is expected to be $\sim 5 \times 10^{-5}$. One can speculate that the substantially larger frequency shift observed in our experiment can be attributed to the Young’s modulus changes of the insulation layers (Kapton, glue) surrounding the conductor, or amplified by thermally induced interfacial contact changes in the stack.

In conclusion, we have proposed and validated an active technique for detecting quenches in HTS conductor stack assemblies based on monitoring their transient acoustic response. We demonstrated a capability to resolve a temperature rise of < 1 K in the conductor quenching inside a stack at 77 K, while the resistive voltage across that conductor was still less than $1 \mu\text{V}$. We believe that our technique has a significant potential for detecting hot spots in larger conductor assemblies, coils, and machinery where such capability is crucial for adequate quench protection. While increasing system size will likely decrease an acoustic wave fraction affected by the thermally perturbed volume, our preliminary tests²⁰ indicate that sensitivity of the technique should be sufficient for detecting quenches in HTS tape windings of at least ~ 100 m in length. A signal-to-noise ratio can be lowered by increasing acoustic wave energy proportionally to system size. Further experiments involving sub-scale HTS coils are currently in progress. The technique can be potentially made spatially selective by band-pass filtering the transient around eigenfrequencies of a specific structural part of the system and may benefit from exploiting acoustic transmission windows of cable stacks and coil windings. In combination with passive acoustic localization,⁵ quench location information can be obtained simultaneously with quench detection, using the same sensor hardware. Also, a large scope of applications may exist in areas beyond superconductor-based devices where fast, non-invasive detection of local temperature changes in the interior of a solid object is required.

This work was supported by the U.S. Department of Energy under Contract No. DE-AC02-05CH11231.

¹F. Trillaud, H. Palanki, U. P. Trociewitz, S. H. Thompson, H. W. Weijers, and J. Schwartz, *Cryogenics* **43**, 271 (2003).

²J. van Nugteren, M.Sc. thesis, University of Twente, 2012.

- ³O. Tsukamoto, J. F. Maguire, E. S. Bobrov, and Y. Iwasa, *Appl. Phys. Lett.* **39**, 172 (1981).
- ⁴O. Tsukamoto and Y. Iwasa, *Adv. Cryog. Eng.* **31**, 259 (1986).
- ⁵M. Marchevsky, G. Sabbi, H. Bajas, and S. Gourlay, *Cryogenics* **69**, 50 (2015).
- ⁶A. Ninomiya, T. Sakaniwa, H. Kado, T. Ishigohka, and Y. Higo, *IEEE Trans. Magn.* **25**, 1520 (1989).
- ⁷T. Ishigohka, O. Tsukamoto, and Y. Iwasa, *Appl. Phys. Lett.* **43**, 317 (1983).
- ⁸F. Scurti, S. Ishmael, G. Flanagan, and J. Schwartz, *Supercond. Sci. Technol.* **29**, 03LT01 (2016).
- ⁹A. M. Mayer, *Philos. Mag* **45**, 18 (1873); M. R. Moldover, R. M. Gavioso, J. B. Mehl, L. Pitre, M. de Podesta, and J. T. Zhang, *Metrologia* **51**, R1 (2014).
- ¹⁰S. Fife, C. D. Andereck, and S. Rahal, *Exp. Fluids* **35**, 152 (2003).
- ¹¹A. S. Birks and R. E. Green, Jr., in *Ultrasonic Testing*, Edited by P. McIntire (American Society for Nondestructive Testing, Columbus, OH, 1991).
- ¹²H. M. Ledbetter, *Cryogenics* **22**, 653 (1982).
- ¹³H. Georgi, *The Physics of Waves* (Prentice-Hall, Inc./A Simon & Schuster Company, Englewood Cliffs, NJ, 1993).
- ¹⁴A. Ninomiya, T. Ishigohka, N. Mizukami, and Y. Higo, *IEEE Trans. Magn.* **24**, 1215 (1988).
- ¹⁵A. Migliori, J. L. Sarrao, W. M. Visscher, T. M. Bell, M. Lei, Z. Fiskl, and R. G. Leisure, *Physica B* **183**, 1 (1993).
- ¹⁶J. P. Den Hartog, *Mechanical Vibrations* (Dover Publications, 2013).
- ¹⁷W. L. Smith and W. J. Spencer, *Rev. Sci. Instrum.* **34**, 268 (1963).
- ¹⁸K. Agatsuma, F. Uchiyama, T. Ohara, K. Tukamoto, H. Tateishi, S. Fuchino, Y. Nobue, S. Ishigami, M. Sato, and H. Sugimoto, *Adv. Cryog. Eng.* **35**, 1563 (1990).
- ¹⁹R. Seip, P. VanBaren, C. A. Cain, and E. S. Ebbini, *IEEE Trans. Ultrason. Ferroelectr. Freq. Control* **43**, 1063 (1996).
- ²⁰M. Marchevsky and S. A. Gourlay, "Active acoustic quench detection for high-temperature superconductor tapes" (to be published).
- ²¹G. A. Levin, P. N. Barnes, and J. S. Bulmer, *Supercond. Sci. Technol.* **20**, 757 (2007).